Quantitative Analysis of Diffusive Reactions at the Solid–Liquid Interface in Finite Systems

ARTICLE *in* JOURNAL OF PHYSICAL CHEMISTRY LETTERS · FEBRUARY 2014

Impact Factor: 7.46 · DOI: 10.1021/jz4024833

4 AUTHORS, INCLUDING:

Thomas C. T. Michaels
University of Cambridge
18 PUBLICATIONS **50** CITATIONS
SEE PROFILE

Alexander Kai Buell
Heinrich-Heine-Universität Düsseldorf
47 PUBLICATIONS **747** CITATIONS
SEE PROFILE

Eugene M Terentjev
University of Cambridge
304 PUBLICATIONS **7,448** CITATIONS
SEE PROFILE

THE JOURNAL OF PHYSICAL CHEMISTRY Letters

Letter

pubs.acs.org/JPCL

Quantitative Analysis of Diffusive Reactions at the Solid−Liquid Interface in Finite Systems

Thomas C. T. Michaels,[†] Alexander K. Buell,[†] Eugene M. Terentjev,*[,‡] and Tuomas P. J. Knowles*[,†]

[†]Department of Chemistry, University of Cambridge, Lensfield Road, Cambridge CB2 1EW, United Kingdom

[‡]Cavendish Laboratory, University of Cambridge, J.J. Thomson Avenue, Cambridge CB3 0HE, United Kingdom

ABSTRACT: A central element in many processes in physics, chemistry and biology is a reaction between a species immobilized on a surface and a partner that is able to diffuse in solution. However, integrated rate laws for this class of chemical processes have so far only been found in certain special cases. Here, we present a model for the time dependence of an irreversible reaction between particles in a solution of finite volume and a surface. The resulting analytical expression allows quantitative analysis of the transient kinetics of the reaction between soluble particles and a surface. We apply this approach to the analysis of quartz crystal microbalance experiments of protein aggregation under conditions where both reaction and diffusion define the overall kinetics. Furthermore, we use the model to determine absolute mass sensitivity coefficients for soft and rough surfaces, a situation where conventional approaches to determine the mass sensitivity *a priori* fail.

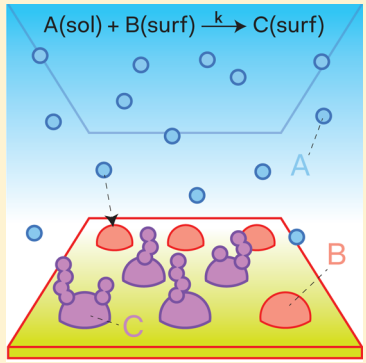

SECTION: Kinetics and Dynamics

Diffusive reactions at solid−liquid interfaces are ubiquitous in many areas of chemistry and physics, such as electrochemistry,[1] Ostwald ripening,[2] electrocrystallization[3] and catalysis,[4] and of biology, such as ligand binding to proteins on cell surfaces,[5] biosensing applications[6] and immunochemical assays.[7] These reactions commonly involve a species immobilized on a surface, reacting with an agent that is able to diffuse freely in solution. Analytical rate laws for the transient kinetics of such processes are available for some specific cases. The most prominent example is the well-known Cottrell equation,[8] which describes the inverse square root behavior of the current with time for fast electrochemical reactions at an infinite planar electrode in contact with a semi-infinite reservoir of soluble electrochemically active species. More recent extensions of the Cottrell equation and related solutions have mainly focused on the description of the effects of finite surface effects[9,10] and inhomogeneous[11] (electrode) surfaces.

In many practically relevant situations the reactions at the solid−liquid interface exhibit finite kinetics due to energy barriers separating the different states. Such barriers can be, for example, due to stuctural rearrangements and desolvation.[12] The theoretical description and modeling of the transient kinetics of such processes therefore need to include the rates of both the diffusion and the reaction. Furthermore, the semi-infinite boundary conditions in the classical Cottrell treatment of electrochemical processes do not adequately describe situations where diffusion and reaction occur in a pore of finite size. The time-dependent diffusion coefficients for such systems have been derived for reversible reactions,[13,14] but an analytical treatment of the reaction rate in finite systems for irreversible reactions has so far not been presented. This situation is, however, often encountered in biosensing and required, for example, for a quantitative analysis of protein aggregation reactions.

In this Letter, we present a simple model for reactions at the solid−liquid interface in a reaction cell with parallel-plate geometry based on classic mean-field reaction−diffusion kinetics. We solve the appropriate boundary value problem (BVP) for the reaction−diffusion equation in the specified geometry and derive an expression for the amount of sorbed species as a function of time. The resulting expression yields the inverse square root limit of time dependence of the Cottrell equation in the limit of fast reactions but allows slower reactions to be analyzed quantitatively in a regime outside of the applicability of the Cottrell equation. We show that this analysis provides a useful practical tool for the analysis of biosensing experiments where amyloid fibrils that are attached to the surface of a quartz crystal microbalance (QCM)[6] are incubated with low concentrations of soluble protein that can elongate the fibrils. The ability to analyze the entire time course of the aggregation reaction allows us to make use of the known boundary conditions for the concentration of soluble protein and hence determine the total mass that has been transferred to the liquid−solid interface. In particular, this analysis yields an absolute mass sensitivity coefficient for QCM that is not available from current theoretical frameworks for rough and soft surfaces that are commonly involved in biophysical systems.

Received: November 17, 2013
Accepted: January 24, 2014
Published: January 24, 2014

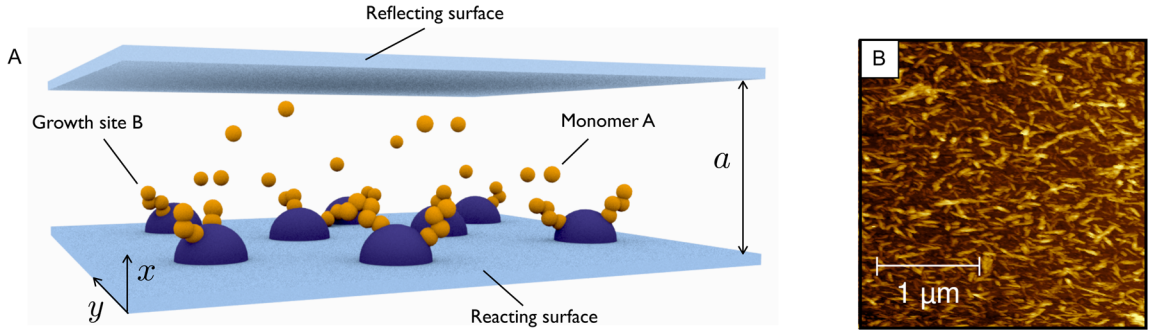

Figure 1. (a) Schematic representation of a reaction A + B → C occurring between a species A in solution and a reactive site B on a surface, for example, growth of surface-bound amyloid fibrils through addition of soluble insulin molecules. (b) Atomic force microcopy (AFM) image of the surface of a QCM sensor with a high density of short insulin amyloid fibrils attached.[6,15] We use the general solution derived in this work to analyze QCM data of the growth of such surface-bound fibrils and to determine the QCM mass sensitivity for such a rough viscoelastic protein layer.

Theory. We consider the reaction between a species in solution A and a reactive site B on a surface described by the reaction scheme

$$\mathrm{A(sol)} + \mathrm{B(surf)} \xrightarrow{k} \mathrm{C(surf)} \tag{1}$$

and proceeding with a rate constant k governing the change in product concentration as a function of time

$$\partial_t|_{\mathrm{reac}}\rho(\vec{x},\,t) = -\partial_t\rho_{\mathrm{C}}(\vec{x},\,t) = -k\rho(\vec{x},\,t)\rho_{\mathrm{B}}(\vec{x},\,t) \tag{2}$$

where ρ denotes the concentration of reacting molecules in solution, ρ_{B} is the concentration of reaction sites on the surface, ρ_{C} is the concentration of the reaction products, and $\vec{x} = (x,y,z)$ (Figure 1a). The reaction scheme in eq 1 describes any irreversible diffusive reaction between species in solution and on the surface and can be used to model a wide range of processes occurring in physical chemistry and biophysics, for example, the reduction of an electrochemical species at a cathode or the growth of amyloid filaments on the surface of a biosensor. Furthermore, our theoretical framework might be extended to describe other processes, such as supported homogeneous catalysis in a regime, where the rate-limiting step is a reaction between a solute and a species immobilized on the surface. Here, we consider the situation in which the reaction sites are homogeneously distributed in the plane $x = 0$ and that their concentration is constant in time, $\rho_{\mathrm{B}}(\vec{x},t) = \delta(x) \cdot (n/A)$, where n/A is the number of reactive sites per unit area on the surface (Figure 1a). The case of constant density of reaction sites corresponds, for instance, to a situation when a metal ion reduced at the cathode becomes electrically connected to the cathode and can in turn capture further cations; similarly, protein molecules that add onto ordered amyloid fibrils attached to a surface (Figure 1b) adopt the configuration of the fibril template and can then promote the attachment of further proteins, that is, the number of capture sites remains unchanged.[6]

The time evolution of the density $\rho(\vec{x},t)$ of particles in solution is obtained from the combined contributions from diffusion $\partial_t|_{\mathrm{diff}}\rho(\vec{x},t) = D\nabla^2\rho(\vec{x},t)$ and the reaction at the surface

$$\partial_t\rho(\vec{x},\,t) = [D\nabla^2 - \tilde{k}\delta(x)]\rho(\vec{x},\,t) \tag{3}$$

where $\tilde{k} = kn/A$ is an effective first-order rate constant. The translational symmetry of the system with respect to the yz-plane implies that we can decompose the density as $\rho(\vec{x},t) = \rho(x,t)\rho_y(y)\rho_z(z)$ and reduce the problem to that of a one-dimensional diffusion[29]

$$\partial_t\rho(x,\,t) = [D\partial_x^2 - \tilde{k}\delta(x)]\rho(x,\,t) \tag{4}$$

We note that k has units of $\mathrm{m^3\ s^{-1}}$ (or alternatively, in chemical convention, $\mathrm{M^{-1}\ s^{-1}} = \mathrm{dm^3\ s^{-1}}$), and therefore, $\tilde{k}$ has units of m/s (or alternatively dm/s) due to the reaction taking place at the solid−liquid interface.

We consider a particle density field $\rho(x,t)$ restricted to a region of space bounded by two reflective walls at $x = \pm a$ with a reacting surface at $x = 0$, the physical region of space corresponding to the space bounded by the $x = 0$ and a planes. Equation 4 is solved subject to the boundary conditions $\partial_x\rho(x = \pm a,t) = 0$ and the initial condition $\rho(x,t = 0) = \rho_0(x)$. With the transformation $D \leftrightarrow -\hbar^2/2m$ and $t \leftrightarrow i\hbar t$, eq 4 is formally equivalent to the time-dependent Schrödinger equation for a single particle evolving in one dimension subject to a delta function potential.[16] The field $\rho(x,t)$ is expanded in terms of the eigenfunctions of the operator $[D\partial_x^2 - k\tilde{\delta}(x)]$ on the right-hand side of eq 4

$$\Phi_q(x) = \cos\left(\frac{q}{\sqrt{D}}|x| + \varphi\right) \tag{5}$$

where $\varphi = \arctan\left(-\tilde{k}/[2q\sqrt{D}]\right)$ is a phase shift that arises from the discontinuity in the first derivative due to the presence of the delta function at $x = 0$ in eq 4. The eigenvalues q satisfy a quantization condition arising from implementing the boundary conditions

$$\frac{q_n}{\sqrt{D}}a = \arctan\left(\frac{\tilde{k}}{2q_n\sqrt{D}}\right) + n\pi \tag{6}$$

for $n = 0,\ 1,\ 2,\ \ldots$. In the case of a uniform initial particle distribution ρ_0, the solution of eq 4 reads

$$\rho(x = 0,\,t) = \rho_0\tilde{k}\sum_{n=0}^{\infty}\frac{\exp(-q_n^2 t)}{aq_n^2 + (a\tilde{k}^2 + 2D\tilde{k})/4D} \tag{7}$$

where q_n are the solutions of eq 6. The reaction rate is obtained from eqs 2 and 7

$$\nu(t) = \tilde{k}\rho(x = 0,\,t) \tag{8}$$

The rate $\nu(t)$ represents the number of particles of type A that successfully bind to the surface, or equivalently the number of product species C that form during the time interval $[t,t + \mathrm{d}t]$

dx.doi.org/10.1021/jz4024833 | J. Phys. Chem. Lett. 2014, 5, 695−699

$$\partial_t \rho_C(x = 0, t) = v(t) \tag{9}$$

The concentration of products C on the surface at time $t > 0$ is thus obtained by integrating eq 8, yielding

$$\rho_C(t) = \rho_0 \tilde{k}^2 \sum_{n=0}^{\infty} \frac{1 - \exp(-q_n^2 t)}{q_n^2 [a q_n^2 + (a\tilde{k}^2 + 2D\tilde{k})/4D]} \tag{10}$$

where q_n denotes the solutions of eq 6. Equation 10 provides a quantitative description of the total concentration of material bound to the surface at time t, a quantity that can be directly compared with experimental observables, such as the total frequency shift in QCM experiments or the change in resonance angle in surface plasmon resonance experiments. We note that similar results have been reported for heat transfer for the case of radiative boundary conditions,[17] as well as in the context of diffusion−collision−coalescence models of protein folding in one dimension.[18] Alternatively, eq 10 is also obtained by integration over the size of the cell of the particle propagator for reversible reactions[14] in the limit of the vanishing backward reaction rate. In the limit of a semi-infinite reservoir, $a \to \infty$, a well-known result of electrochemistry[19] is obtained as a special case of eq 10

$$v(t) = \rho_0 \tilde{k}\, \mathrm{erfc}\left(\frac{\tilde{k}\sqrt{t}}{2\sqrt{D}}\right) \exp\left(\frac{\tilde{k}^2 t}{4D}\right) \tag{11}$$

where $\mathrm{erfc}(x)$ denotes the complementary error function; Figure 2 shows a comparison between the behavior described

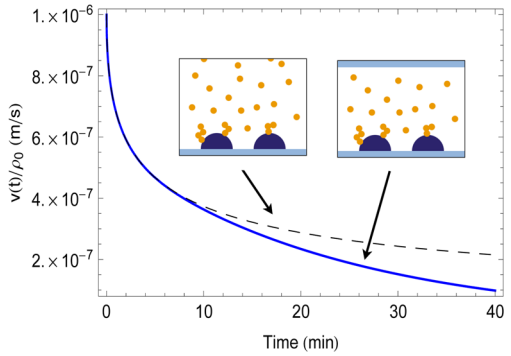

Figure 2. A comparison between a semi-infinite and a finite system. Solid line: reaction rate from eq 7. Dashed line: early time solution to eq 11. The parameters are $a = 0.6$ mm, $\tilde{k} = 10^{-6}$ m/s, $D = 10^{-10}$ m^2/s.

by eqs 7 and 11. In this regime, eq 10 approaches the characteristic inverse square root behavior with time described by the Cottrell equation,[8] $v(t) = 2\rho_0 D^{1/2}/(\pi t)^{1/2}$, during the later stages of the reaction, when the system eventually goes over to a diffusion regime, independently of the relative magnitude of the reaction rate constants and diffusion times.

In the situation where a surface is in contact with a finite solution volume, eq 11 is recovered for the reaction rate only in the early time limit $t \ll a^2/D$, where a^2/D is the average diffusion time from the cell end, with $\tilde{k}$ being replaced by an effective reaction rate constant $\tilde{k}(1 + 2D/a\tilde{k})^{1/2}$ that depends on the size of the system. During the later stages of the reaction, however, qualitatively different behavior is observed, with the concentration of reacting particles at the reacting surface being exponentially suppressed due to quantitative depletion. Equation 10 correctly contains both limits.

Experimental Results. The availability of the general rate law derived in this work opens up the possibility to analyze quantitatively experiments between immobilized and soluble species in a range of geometries, concentrations, and rate constants commonly encountered in biological systems. As an example, here, we analyze data from biosensing experiments of amyloid fibril growth. We have shown previously that this reaction is characterized by substantial free-energy barriers, such that diffusion toward the surface and surface reaction are characterized by similar time scales and that under appropriate conditions, the soluble protein in contact with the surface-bound amyloid fibrils can be quantitatively depleted.[12] Figure 3a shows an experiment where a sensor was exposed to two different concentrations of soluble insulin (1.4 and 0.7 μM). The curves show the expected linear scaling with the initial concentration of soluble protein, ρ_0. Depletion curves were fitted using the first 10 terms in eq 10 with the measured values of $a = 0.6$ mm and $D = 2.4 \times 10^{-10}$ m^2/s at $T = 55$ °C as inputs.

Next, we wanted to test whether the effects on the measured frequency traces of selective changes in important system parameters could be accurately predicted by our rate law. The variable pertinent from an experimental point of view in this context is the rate constant, k. The diffusion coefficient D cannot be changed without also affecting k due to the diffusive nature of the kinetic prefactor $\Gamma = D\rho r_{\mathrm{eff}}$ (in the limit of low concentrations ρ) in the expression for the rate constant $k = \Gamma e^{-\beta \Delta G^{\ddagger}}$.[20] The converse, however, does not apply, and if the free-energy barrier $\Delta G^{\ddagger}$ of fibril growth is modified, only k will change. A convenient way to change the rate constant is through tuning of the electrostatic interactions between the surface-bound growth-competent seed fibrils and the soluble protein. This is most readily achieved via a change in ionic strength that affects the electrostatic screening.[21] Importantly, an increase in salt concentration from an initial concentration of 100 mM at the low protein concentrations used in our experiments (μM) will not change the diffusion coefficient of the protein molecules due to the fact that the Debye screening length is much shorter at these salt concentrations than the average distance between protein molecules. The rate constant k could also be changed through a change in temperature,[20] but this would also affect the diffusion coefficient D. Finally, we note that k can be modified through changes in protein sequence that modify the free-energy barrier $\Delta G^{\ddagger}$ without affecting D;[22] however, here we adopt the simplest possible approach, that is, a modification of the electrostatic part of the free-energy barrier $\Delta G^{\ddagger}$ through an increase in the concentration of NaCl. In order to assess the relative rate constants k independently at three different concentrations of NaCl, we performed experiments at high concentrations of soluble protein where no depletion effects are observed and where the observed rate of change of frequency is linear over hours. In this regime, the relative rate constants k at 100, 200, and 300 mM NaCl were found to scale as 1:2.08:2.34, in close agreement with previous results.[21] Figure 3b shows the three depletion curves corresponding to these conditions. All parameters, except k, were identical in the three experiments. The slowest depleting curve is a fit, and the two others are predictions based on the relative rates measured as described above.

Finally, we can use the rate law to provide an absolute mass sensitivity of QCM sensors for rough and soft adlayers such as those that arise from the growth of surface-bound amyloid fibrils. For this type of system, there is currently no a priori

dx.doi.org/10.1021/jz4024833 | J. Phys. Chem. Lett. 2014, 5, 695−699

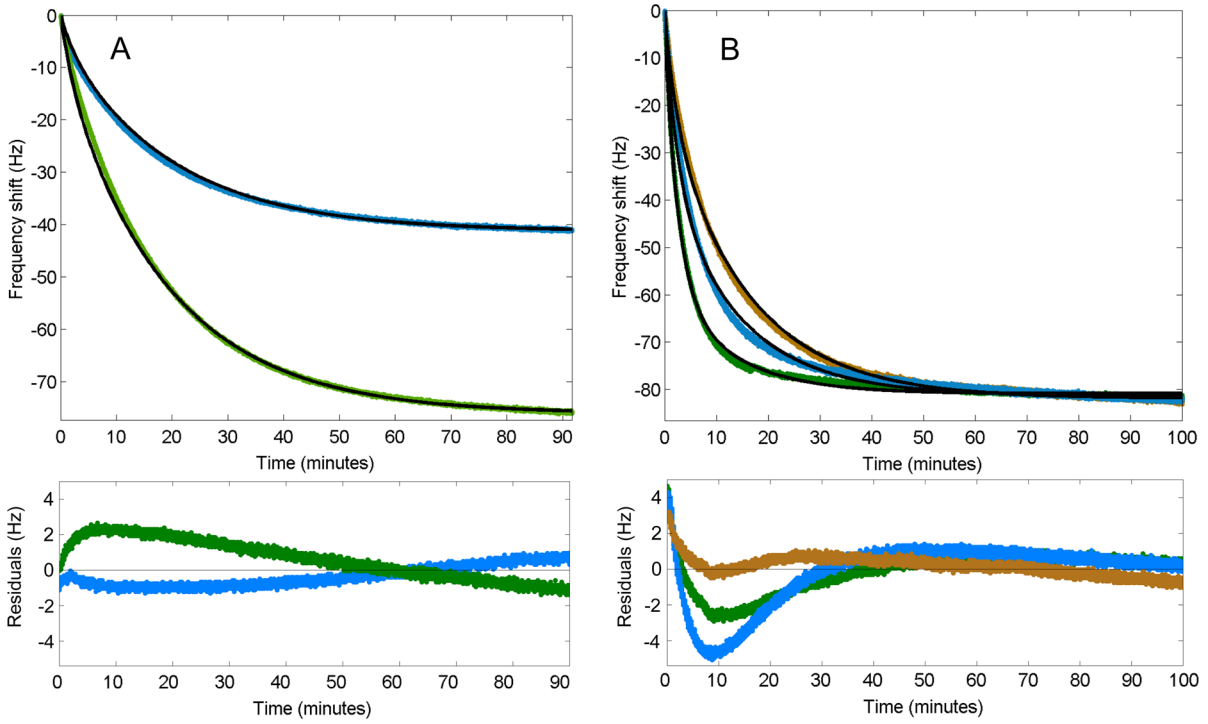

Figure 3. Experimental data obtained from QCM measurements of amyloid elongation (color line), fit using the model eq 10 (black line) and residual plots (bottom panels). (a) The two curves correspond to two different initial concentrations of soluble protein, 1.4 (bottom curve) and 0.7 μM (top curve). The curves were fitted using the first 10 terms in eq 10. (b) Depletion curves for three different effective rate constants k, adjusted via a change in solution ionic strength (from right to left: 100, 200, and 300 mM of added NaCl). The rate constants for the three measurements satisfy the relation $k_1/k_2/k_3 = 1: 2.08: 2.34$. The fitting was obtained as follows. The 100 mM curve was fitted with $\tilde{k} = 3.06 \times 10^{-6}$ m/s. The other fits are predictions obtained with $2.08\tilde{k}$ and $2.34\tilde{k}$, respectively. The parameters of the system are $a = 0.6$ mm and $D = 2.4 \times 10^{-10}$ m^2/s at $T = 55$ °C.

method available to determine the mass sensitivity; however, this quantity is a key parameter for the quantitative analysis of QCM data of rough adlayers.[6,23] We exploit the fact that the total dry mass of protein that has attached to the sensor can be determined from the fits in Figure 3 because the rate law connects the initial condition of known soluble monomer to the final state where all of the soluble protein has reacted. We use this approach to determine the mass sensitivity under the conditions of the experiment shown in Figure 3a to be $C_f \approx 4$ ng/Hz for the frequency overtone is $N = 3$, which is shown in Figure 3a. The fundamental frequency is often not analyzed in QCM experiments as it is most prone to noise due to incomplete energy trapping.[24] This value is approximately four times as high as the mass sensitivity predicted by the Sauerbrey equation ($C_f = 17.7$ ng/Hz).[25] The mass sensitivity for amyloid fibril growth depends on the frequency overtone and varies between 4 ($N = 3$) and 6.5 ng/Hz ($N = 13$) under the conditions of the experiments in Figure 3a. The higher mass sensitivity compared to the Sauerbrey case reveals the role of solvation water of the proteins and water trapped between the fibrils.[26]

In the present work, we reported on a theoretical and experimental study of particle depletion in diffusive reactions at surfaces. We presented a simple model of particles diffusing in a slit pore and irreversibly reacting with sites immobilized on a surface. The model has allowed us to analyze quantitatively biosensing data outside of the regime where conventional limiting cases for rate laws for reactions at surfaces are applicable, providing the corresponding surface reaction rate constant. Furthermore, we have been able to use the obtained rate law to determine the absolute mass sensitivity for QCM measurements on soft and rough surfaces, a situation for which conventional approaches to determine mass sensitivity a priori fail. We anticipate that similar analysis would allow analysis of biosensing or electrochemical data in a variety of other contexts where confinement plays a key role, including inside of living cells.[27]

EXPERIMENTAL METHODS

A detailed protocol for the QCM experiments can be found in ref 28. The QCM experiments were carried out with a QCM-D E4 (Q-Sense, Västra Frölunda, Sweden). Bovine insulin (M = 5.7 kDa) was purchased from Seralab (Haywards Heath, U.K.). Insulin seed fibril formation and the attachment to the gold-coated QSX 301 sensors was carried out as described previously.[15] In order to achieve sufficiently fast kinetics, the experiments were carried out at 50 or 55 °C. The QCM instrument was introduced into a thermostatted chamber, the temperature of which was adjusted to within 2 °C of the desired temperature, and the Peltier element of the QCM stabilized the instrument's temperature to within 0.05 °C of the desired value. Protein stock solutions were prepared in 10 mM HCl at ~1 mg/mL (measured by absorption at 280 nm, using an absorption coefficient of 5840 M^{-1} cm^{-1}), and 100−300 mM NaCl was added. For injection, the protein solutions were diluted to concentrations on the order of 1 μM, corresponding to a total mass of protein in the flow cell on the order of 200 ng. Before injection of the dilute protein solutions into the liquid cell of the QCM, the seed fibrils were exposed to 10 mM HCl with the same concentration of NaCl as that in the protein solution in order to avoid frequency shifts due to density differences of the solutions and induced structural changes of

dx.doi.org/10.1021/jz4024833 | J. Phys. Chem. Lett. 2014, 5, 695−699

the seed fibrils. The protein solutions were introduced into the liquid cell of the QCM (height 0.6 mm) with a peristaltic pump at a flow rate of 200 μL/min. The pump was stopped after 90 s, when the flow system and the liquid cell had been filled with the protein solution, and the system was left undisturbed until the rate of change of the frequency shift had reached zero. The frequency traces (the overtone $N = 3$ was analyzed) were fitted as shown in Figure 3. The curves in Figure 3 were normalized to the same final level due to the fact that the mass sensitivity was found to exhibit some dependency on the density of the solution and on small differences in the structure and density of the fibrils induced by differences in ionic strength. In order to exclude the presence of convective processes in the liquid cell of the QCM, which would complicate the analysis of the frequency traces, we performed a depletion experiment with the QCM setup inverted. In the case of non-negligible convection, this would lead to a difference in the frequency trace compared to the case where the instrument is in its normal configuration. We observed no difference between the two situations (data not shown) and therefore conclude that convective processes can be neglected.

AUTHOR INFORMATION

Corresponding Authors

*E-mail: emt1000@cam.ac.uk (E.M.T.).
*E-mail: tpjk2@cam.ac.uk (T.P.J.K.).

Notes

The authors declare no competing financial interest.

ACKNOWLEDGMENTS

This work has been supported by St. John's College, Cambridge (T.C.T.M., T.P.J.K.), Magdalene College, Cambridge (A.K.B.), the Leverhulme Trust (A.K.B.), and the Newman foundation. We thank Q-Sense for the loan of the QCM instrument, J. B. Kirkegaard and S. Matis for helping with figures, B. Schlein and E. Maisonhaute for helpful discussions.

REFERENCES

(1) Amatore, C.; Savant, J.; Tessier, D. Charge Transfer at Partially Blocked Surfaces: A Model for the Case of Microscopic Active and Inactive Sites. *J. Electroanal. Chem.* **1983**, *147*, 39−51.

(2) Voorhees, P.; Glicksman, M. Solution to the Multi-Particle Diffusion Problem with Applications to Ostwald Ripening — I. Theory. *Acta Metall.* **1984**, *32*, 2001−2011.

(3) Sluyters-Rehbach, M.; Wijenberg, J.; Bosco, E.; Sluyters, J. The Theory of Chronoamperometry for the Investigation of Electrocrystallization. *J. Electroanal. Chem.* **1987**, *236*, 1−20.

(4) Sherwood, T. Diffusion Phenomena in Heterogeneous Catalysis. *Pure Appl. Chem.* **1965**, *10*, 595−610.

(5) Zwanzig, R.; Szabo, A. Time Dependent Rate of Diffusion-Influenced Ligand Binding to Receptors on Cell Surfaces. *Biophys. J.* **1991**, *60*, 671−678.

(6) Knowles, T. P. J.; Shu, W.; Devlin, G. L.; Meehan, S.; Auer, S.; Dobson, C. M.; Welland, M. E. Kinetics and Thermodynamics of Amyloid Formation from Direct Measurements of Fluctuations in Fibril Mass. *Proc. Natl. Acad. Sci. U.S.A.* **2007**, *104*, 10016−10021.

(7) Nygren, H.; Stenberg, M. Immunochemistry at Interfaces. *Immunology* **1989**, *66*, 321−327.

(8) Cottrell, F. Der Reststrom bei Galvanischer Polarisation, Betrachtet als ein Diffusionsproblem. *Z. Phys. Chem.* **1902**, *42*, 385−431.

(9) Soos, Z. G.; Lingane, P. J. Derivation of the Chronoamperometric Constant for Unshielded, Circular, Planar Electrodes. *J. Phys. Chem.* **1964**, *68*, 3821−3828.

(10) Aoki, K.; Osteryoung, J. Diffusion-Controlled Current at the Stationary Finite Disk Electrode: Theory. *J. Electroanal. Chem. Interfacial Electrochem.* **1981**, *122*, 19−35.

(11) Davies, T. J.; Banks, C. E.; Compton, R. G. Voltammetry at Spatially Heterogeneous Electrodes. *J. Solid State Electrochem.* **2005**, *9*, 797−808.

(12) Buell, A. K.; Dhulesia, A.; White, D. A.; Knowles, T. P. J.; Dobson, C. M.; Welland, M. E. Detailed Analysis of the Energy Barriers for Amyloid Fibril Growth. *Angew. Chem., Int. Ed.* **2012**, *51*, 5247−5251.

(13) Dudko, O. K.; Berezhkovskii, A. M.; Weiss, G. H. Time-Dependent Diffusion Coefficients in Periodic Porous Materials. *J. Phys. Chem. B* **2005**, *109*, 21296−21299.

(14) Levesque, M.; Bnichou, O.; Rotenberg, B. Molecular Diffusion Between Walls with Adsorption and Desorption. *J. Chem. Phys.* **2013**, *138*, 034107/1−034107/3.

(15) Buell, A. K.; White, D. A.; Meier, C.; Welland, M. E.; Knowles, T. P. J.; Dobson, C. M. Surface Attachment of Protein Fibrils via Covalent Modification Strategies. *J. Phys. Chem. B* **2010**, *114*, 10925−10938.

(16) Gaveau, B.; Schulman, L. S. Explicit Time-Dependent Schrödinger Propagators. *J. Phys. A: Math. Gen.* **1986**, *19*, 1833−1846.

(17) Carslaw, H.; Jaeger, J. *Conduction of Heat in Solids*; Oxford University Press: New York, 1959.

(18) Karplus, M.; Weaver, D. L. Diffusion−Collision Model for Protein Folding. *Biopolymers* **1979**, *18*, 1421−1437.

(19) Bard, A. J.; Faulkner, L. R. *Electrochemical Methods: Fundamentals and Applications*; John Wiley & Sons: New York, U.S..; 2001.

(20) Buell, A. K.; Blundell, J. R.; Dobson, C. M.; Welland, M. E.; Terentjev, E. M.; Knowles, T. P. J. Frequency Factors in a Landscape Model of Filamentous Protein Aggregation. *Phys. Rev. Lett.* **2010**, *104*, 228101−228105.

(21) Buell, A. K.; Hung, P.; Salvatella, X.; Welland, M. E.; Dobson, C. M.; Knowles, T. P. J. Electrostatic Effects in Filamentous Protein Aggregation. *Biophys. J.* **2013**, *104*, 1116−1126.

(22) Buell, A. K.; Dhulesia, A.; Mossuto, M. F.; Cremades, N.; Kumita, J. R.; Dumoulin, M.; Welland, M. E.; Knowles, T. P. J.; Salvatella, X.; Dobson, C. M. Population of Nonnative States of Lysozyme Variants Drives Amyloid Fibril Formation. *J. Am. Chem. Soc.* **2011**, *133*, 7737−7743.

(23) Chen, R. J.; Bangsaruntip, S.; Drouvalakis, K. A.; Kam, N. W. S.; Shim, M.; Li, Y.; Kim, W.; Utz, P. J.; Dai, H. Noncovalent Functionalization of Carbon Nanotubes for Highly Specific Electronic Biosensors. *Proc. Natl. Acad. Sci. U.S.A.* **2003**, *100*, 4984−4989.

(24) Johannsmann, D. Viscoelastic Analysis of Organic Thin Films on Quartz Resonators. *Macromol. Chem. Phys.* **1999**, *200*, 501−516.

(25) Sauerbrey, G. Verwendung von Schwingquarzen zur Wägung Dünner Schichten und zur Mikrowägung. *Z. Phys. A: Hadrons Nucl.* **1959**, *155*, 206−222.

(26) Macakova, L.; Blomberg, E.; Claesson, P. M. Effect of Adsorbed Layer Surface Roughness on the QCM-D Response: Focus on Trapped Water. *Langmuir* **2007**, *23*, 12436−12444.

(27) Wang, Y.; Nol, J.-M.; Velmurugan, J.; Nogala, W.; Mirkin, M. V.; Lu, C.; Collignon, M. G.; Lemaître, F.; Amatore, C. Nanoelectrodes for Determination of Reactive Oxygen and Nitrogen Species Inside Murine Macrophages. *Proc. Natl. Acad. Sci. U.S.A.* **2012**, *109*, 11534−11539.

(28) Buell, A. K.; Dobson, C. M.; Welland, M. E. In *Amyloid Proteins: Methods and Protocols*; Sigurdsson, E. M., et al., Eds.; Methods in Molecular Biology; Humana Press: New York, 2012; Vol. *849*.

(29) We note that in the practical cases cited as examples in this Letter, the surface density of binding sites is usually high enough, such that the assumption of planar diffusion towards the surface is satisfied.